

ϕ^3 Analyticity and Finite-Energy Sum Rule For Inclusive Reactions

A. I. SANDA
National Accelerator Laboratory, Batavia, Illinois 60510

ABSTRACT

Using ϕ^3 theory as a model, the analytic structure of the six-point function is investigated in the kinematical region appropriate to inclusive reactions. With some idea about the analyticity, a finite-energy sum rule is derived. This sum rule can be used to study the concept of generalized duality. The most striking feature of the sum rule is a possibility that the "triple-Regge vertex function" can be calculated by the data on the inclusive reaction with relatively low M^2 , i. e., the resonance production region.



I. INTRODUCTION

It has been conjectured that the cross section for

$$a + b \rightarrow c + \text{anything} \quad (1)$$

is related to the absorptive part of a scattering amplitude for

$$a + b + \bar{c} \rightarrow a + b + \bar{c} \quad (2)$$

when later is analytically continued to the proper kinematical region.¹

Then various asymptotic behaviors of (1) can be obtained from that

of (2). It is assumed that the asymptotic behaviors of (2) can be

obtained by the $0(2,1)$ expansion.² Subsequently, it has been

verified in the context of field theory that the amplitude for the reaction

(2), when continued analytically, indeed has the absorptive part which is

proportional to the cross section for the reaction (1).³

We see the analogy between the four-point function and the six-point function developing. The inclusive cross section and the six-point function satisfy a relationship similar to that between the total cross section and the four-point function. The $0(2,1)$ expansion in the six-point function corresponds to the Regge expansion in the four-point function. We therefore see that machinery developed for the four-point function (Forward-dispersion relations, Finite-energy sum rules, etc.) may be perhaps applicable to the six-point function. What follows is the first attempt along this line.

In order to start the program, we must first get some idea about the analyticity. No doubt the problem of analyticity and crossing for

the six-point function will be complicated. At present we can gain insight only by investigating a reliable model. For this purpose, we will use ϕ^3 theory as our guide.

The kinematical variables for our problem are

$$\begin{array}{ll} S = (p_a + p_b)^2 & p_a^2 = m^2 \\ t = (p_a - q)^2 & p_b^2 = m^2 \\ M^2 = (p_a + p_b - q)^2 & q^2 = \mu^2 \end{array}$$

where the momenta are defined by Fig. 1.

The result of our analysis indicates that the analyticity on the M^2 plane for fixed $t \leq 0$ and large s and s/M^2 is directly related to the analyticity in the mass variable of an ordinary Regge residue function. Given the possibility that there might be some complex branch point on the M^2 plane in addition to the singularity obtained from unitarity, we must be cautious in applying analytic-function theory to the scattering amplitude. We will, however, assume, for now, that such complex branch points are absent. This assumed analyticity, together with ideas about triple-Regge dominance, yields a sum rule which corresponds to the finite-energy sum rule for the four-point function.

In Sec. II. we discuss the optical theorem for the six-point function. In Sec. III we consider possibilities for complex cuts and state a theorem on the analyticity of the relevant Feynman diagram. In Sec. IV. we

prove the theorem. This section can be skipped without loss of continuity. In Sec. V we derive a finite-energy sum rule. In Sec. VI we present sum rules which require additional assumption about fixed poles, etc.

II. GENERALIZED OPTICAL THEOREM

The cross section for reaction (1) can be written as

$$\frac{d\sigma}{dt d^4x} = \frac{m^2}{(2\pi)^2 S^2} A(s, t, M^2)$$

$$A(s, t, M^2) = \lim_{\Gamma \rightarrow \mu^+} \frac{E_a E_b}{m^2} \int d^4x e^{-i q \cdot x} (q^2 - \mu^2)^2 \langle p_a p_b^{out} | \phi_c(x) \phi_c(0) | p_a p_b^{in} \rangle$$

where $\phi_c(x)$ is the field operator for the particle c. Let T be the amplitude for the process shown in Fig. 2.

$$T = \lim_{\Gamma \rightarrow \mu^+} \frac{E_a E_b}{m^2} \int d^4x e^{-i q \cdot x} (q^2 - \mu^2)(q^2 - \mu^2) \langle p_a p_b^{out} | T(\phi_c(x) \phi_c(0)) | p_a p_b^{in} \rangle \quad (3)$$

T is a function of 25 Lorentz scalars that can be constructed out of the six four vectors and thus it has singularities for 25 different channels.⁴

It has been shown that in the forward limit when s and t are fixed, $s > s$ -channel threshold, $t < 0$, the absorptive part of T in M^2 is proportional to A . We would like to sketch the reasoning behind above statement. Let us first define what we mean by the forward limit. Since the limit is used to relate the cross section to the absorptive part of T , all the four vectors must approach a real limit. That is $\lim p_i = \lim p'_i =$ real four vector, $\lim q = \lim q' =$ real four vector. But it is important to keep in mind that the direction and the rate at which these four vectors approach the limit is not specified. For example, in the special frame in which $\vec{p}_a = 0$, we can have

$$\begin{aligned}
 p_a &= (\epsilon, 0, 0, 0) & , & & p'_a &= (m, 0, 0, 0) \\
 p_b &= (E + \epsilon E_b, 0, 0, \sqrt{E^2 - m^2}) & , & & p'_b &= (E - \epsilon E'_b, 0, 0, \sqrt{E^2 - m^2}) \\
 q &= (q_0 + i\epsilon, q_x, 0, q_z) & , & & q' &= (\epsilon + i\epsilon', q_x, 0, q_z)
 \end{aligned}$$

In the forward limit, all ϵ 's approach zero. But it is our choice as to how they go to zero. For what follows, we make the distinction between primed and unprimed variables only if it is important to keep track of $i\epsilon$'s. In the forward limit when s and t are fixed and $s > s$ -channel threshold, $t < 0$, only those variables that are linearly related to $p_b \cdot q$, $p_b \cdot q'$, or $p'_b \cdot q$ can vary. They are

$$\begin{aligned}
 M^2 &= (p_s + p_e - q)^2 \\
 M_1^2 &= (p_s + p'_e - q)^2 = 2t + 2m^2 - M^2 \\
 M_2^2 &= (p_s - t_e + q)^2 = s + s' + 2\mu^2 - M^2 \\
 M_3^2 &= (-p'_s + p_e - q)^2 = 6m^2 + 2\mu^2 - s - s' - 2t + M^2 \\
 \chi_4 &= (p_e - q)^2 = 2m^2 + \mu^2 + M^2 - s - t \\
 \chi_5 &= (p'_e - q)^2 = 2m^2 + \mu^2 + M^2 - s' - t \\
 \chi_7 &= (p_e + q)^2 = s' + \mu^2 - M^2 + t \\
 \chi_8 &= (p'_e + q)^2 = s + \mu^2 - M^2 + t
 \end{aligned} \tag{4}$$

where we have set $p_a^2 = p_b^2 = m^2$. These channels are shown in Fig. 3.

The absorptive part in M^2 , when $s = s_0 + i\epsilon_1$, $s' = s_0 + i\epsilon_2$, t real is

$$\begin{aligned}
 2i A_{ba} T &= T (s = s_0 + i\epsilon_1, s' = s_0 + i\epsilon_2, t, M^2 = M_0^2 + i\epsilon_3) \\
 M_1^2 &= 2t + 2m^2 - M_0^2 - i\epsilon_3, M_2^2 = 2s_0 + 2\mu^2 - M_0^2 - i(\epsilon_1 + \epsilon_2 + \epsilon_3), \\
 M_3^2 &= 6m^2 + 2\mu^2 - 2s_0 - 2t + M_0^2 + i(-\epsilon_1 - \epsilon_2 + \epsilon_3) \\
 \chi_7 &= s_0 + \mu^2 + t - M_0^2 + i(\epsilon_2 - \epsilon_3), \chi_8 = s_0 + \mu^2 + t + i(\epsilon_1 - \epsilon_2), \\
 \chi_4 &= -s_0 + M_0^2 + 2m^2 + \mu^2 - t + i(\epsilon_1 + \epsilon_3), \chi_5 = -s_0 + M_0^2 + 2m^2 + \mu^2 - t + i(\epsilon_2 + \epsilon_3) \\
 &- T (s = s_0 + i\epsilon_1, s' = s_0 + i\epsilon_2, M^2 = M_0^2 - i\epsilon_3, t) \\
 M_1^2 &= 2t + 2m^2 - M_0^2 + i\epsilon_3, M_2^2 = 2s_0 + 2\mu^2 - M_0^2 + i(\epsilon_1 + \epsilon_2 + \epsilon_3) \\
 M_3^2 &= 6m^2 + 2\mu^2 - 2s_0 - 2t + M_0^2 + i(\epsilon_1 - \epsilon_2 - \epsilon_3) \\
 \chi_7 &= s_0 + \mu^2 + t - M_0^2 + i(\epsilon_2 + \epsilon_3), \chi_8 = s_0 + \mu^2 + t + i(\epsilon_1 + \epsilon_3), \\
 \chi_4 &= -s_0 + M_0^2 + 2m^2 + \mu^2 - t + i(-\epsilon_1 - \epsilon_3), \chi_5 = -s_0 + M_0^2 + 2m^2 + \mu^2 - t + i(\epsilon_2 - \epsilon_3)
 \end{aligned} \tag{5}$$

Note that if we choose $\epsilon_1, \epsilon_2, \epsilon_3$ such that $|\epsilon_1| > |\epsilon_3|, |\epsilon_2| > |\epsilon_3|$ only the discontinuity in M^2 and M_1^2 contributes to the difference. All other channel variables are evaluated in the same side of their respective cuts. (That is, small imaginary part for all variables, except M^2 and M_1^2 does not change sign between two terms on the right-hand side of Eq. 5, the unitarity equation. In other words T has singularities corresponding to each channel associated with variables listed in footnote 4, but it is possible to isolate a sheet on the M^2 plane which contains only the singularities due to the M^2 and M_1^2 channels. From now on "M² plane" refers to this sheet. The absorptive part of T in M^2 can be evaluated from Eq. 3.

$$\begin{aligned}
 & \text{Abs}_{M^2} T(s = s_0 + i\epsilon_1, s' = s_0 + i\epsilon_2, t, p^{\text{in}}) \\
 &= \lim_{q^2 \rightarrow p^2} \sum_n \frac{E_n E_n}{m^2} (q^2 - p^2)^2 (2\pi)^4 \\
 & \times \left[\delta^+(p_a + p_b - q - p_n) \langle p_a p_b^{\text{out}} | \phi_c^+(s) | n \rangle \langle n | \phi_c(s) | p_a p_b^{\text{in}} \rangle \right. \\
 & \quad \left. + \delta^+(p_a - p_b' - q - p_n) \langle p_a p_b^{\text{out}} | \phi_c^+(s) | n \rangle \langle n | \phi_c(s) | p_a p_b^{\text{in}} \rangle \right]
 \end{aligned}$$

Note that the first term on the right hand side is non-zero only if

$p_a + p_b - q = p_n$ and the second term is non zero only if $p_a - p_b' - q = p_n$.

These two regions do not overlap. Consider the region where

$p_a + p_b - q = p_n$. We want to show that

$$A \lim_{s \rightarrow M^2} T(s = s_0 + i\epsilon_1, s' = s_0 - i\epsilon_1, t, M^2) = A \quad (6)$$

where

$$A = \lim_{q^2 \rightarrow \mu^2} \sum_n \frac{E_a E_b}{m^2} (q^2 - \mu^2)^2 (2\pi)^4 \times \delta^4(p_a + p_b - q - p_n) \langle p_a p_b | f_c^\dagger(\omega) | n \rangle \langle n | f_c(\omega) | p_a p_b \rangle.$$

Of course the distinction between Abs T and A are "in" and "out" states.

Let us define an analytic function $F(s, M^2, t)$ such that

$$\lim_{\epsilon_1, \epsilon_3 \rightarrow 0} F_n(s_0 + i\epsilon_1, M^2 + i\epsilon_3, t) = \sqrt{\frac{E_a E_b}{m^2}} \langle p_a, p_b^{\text{out}} | \phi_c^\dagger(\omega) | n \rangle$$

Then Eq. 6 is proven if we can show that

$$\lim_{\epsilon_1, \epsilon_3 \rightarrow 0} F_n(s_0 - i\epsilon_1, M^2 + i\epsilon_3, t) = \sqrt{\frac{E_a E_b}{m^2}} \langle n | \phi(\omega) | p_a p_b \rangle^\dagger \quad (7)$$

since the continuation of T from $s' = s_0 + i\epsilon_1$ to $s' = s_0 - i\epsilon_1$ is given

by the continuation of F_n from $s' = s_0 + i\epsilon_1$ to $s' = s_0 - i\epsilon_1$. Let $t < 0$ be

below the t-channel threshold. By reducing b we obtain

$$\begin{aligned} \sqrt{\frac{E_a E_b}{m^2}} \langle p_a | p_b^{\text{out}} | \phi^+(0) | n \rangle &= \lim_{\substack{\epsilon_1 \rightarrow 0 \\ \epsilon_2 \rightarrow 0}} F(s_0 + i\epsilon_1, M^2 + i\epsilon_2, t) \\ &= \lim_{\substack{\epsilon_1 \rightarrow 0 \\ \epsilon_3 \rightarrow 0}} \lim_{p_b^0 \rightarrow m_b^0} \int d^3x e^{-i\vec{p}_b \cdot \vec{x}} (p_b^2 - m^2) \times \end{aligned} \tag{8}$$

$$\begin{aligned} & \left[\langle p_a | \phi_b(\vec{x}, 0) \frac{1}{p_b^0 + p_a^0 - H - i\epsilon} \phi_c^+(0) | n \rangle \right. \\ & \left. + \langle p_a | \phi_c^+(0) \frac{1}{p_b^0 - p_a^0 - H - i\epsilon} \phi_b(\vec{x}, 0) | n \rangle \right] \end{aligned}$$

where we have performed the x_0 integration by using an integral representation for the theta function. If we evaluate Eq. 8 in the rest frame of a, $s = 2(m^2 + mE + im\epsilon_b + iE\epsilon_b)$, the continuation to the opposite side of the cut in s is equivalent to continuing p_b^0 to the other side of its cut. On the other side of the cut in p_b^0 , the sign of $i\epsilon$ changes

$$\begin{aligned} F(s_0 - i\epsilon_1, M^2 + i\epsilon_2, t) &= \\ & \lim_{\substack{\epsilon_1 \rightarrow 0 \\ \epsilon_2 \rightarrow 0}} \frac{E_a}{m} \int d^3x e^{-i\vec{p}_b \cdot \vec{x}} (p_b^2 - m^2) \times \\ & \left[\langle p_a | \phi_b(\vec{x}, 0) \frac{1}{p_b^0 + p_a^0 - H + i\epsilon} \phi_c^+(0) | n \rangle \right. \\ & \left. + \langle p_a | \phi_c^+(0) \frac{1}{p_b^0 - p_a^0 - H + i\epsilon} \phi_b(\vec{x}, 0) | n \rangle \right] \end{aligned}$$

If b is reduced in $\sqrt{\frac{E_a E_b}{m_a m_b}} \langle n | \phi(0) | p_a p_b^{\text{in}} \rangle$, it is quite easily seen that indeed Eq. 7 holds.

We stress again the most important point that there is a sheet in M^2 plane which contains only the M^2 and M_1^2 channel singularities.

If the singularities from the other channels can not be separated, there is no simple relation between the cross section for the inclusive reaction and the absorptive part of the six-point function. Let us take a particular example $a = \pi^-$, $b = \text{proton}$, and $c = K^-$. The process which gives the right hand cut, shown in Fig. 3a, is non zero when

$$M^2 \geq (\mu_K + m)^2$$

(For

the left hand cut see below). The break in the cut is due to the requirement that $q^2 = \mu_K^2$. The cut in the region $(\mu_K + m_p)^2 \leq M^2 \leq (\sqrt{s} - \mu_K)^2$ corresponds to the emission of K as it can easily be verified that $q_0 \geq \mu_K$. The cut in the region $M^2 \geq (\sqrt{s} + \mu_K)^2$ corresponds to the three-particle scattering process since $q_0 \leq -\mu_K$, provided s and s' are analytically continued to the proper side of the cut.

The second term in Eq. 7 is shown in Fig. 3b. We are interested in the case where s and s' are held fixed and large. In particular $(p_a - q)^2 = t < 0$, $(p_a - p_b')^2 \approx -s < 0$, $(q + p_b')^2 = s + \mu^2 - M^2 + t$. Then this diagram corresponds to the cross section for the inclusive process $K^- + p \rightarrow \pi^- + \text{anything}$ and the scattering process $K^- + \pi^+ + p \rightarrow \text{anything}$.

The incident energy for these two reactions are $(p_b + q') = s + \mu^2 - M^2 + t$ and M^2 respectively. The momentum transfer between π and K is t . The cut on the M^2 plane corresponding to this process is located at the position

$$M_1^2 = 2t + 2m^2 - M^2 \geq (m_\Sigma + \mu_\pi)^2, \quad M_1^2 \geq m_\Sigma^2.$$

This cut corresponds to the left hand cut shown in Fig. 4.

III. COMPLEX CUTS?

So far we have been discussing the singularities whose existence is guaranteed by unitarity. Are there any other singularities? It is our task to investigate the additional singularity structure of the amplitude T , besides the cuts shown in Fig. 4, in the region $|M^2| \leq (\sqrt{s} - \mu_\pi)^2$. We do not have to look far to find such singularities. In fact a box diagram shown in Fig. 5 will give a complex branch point on the physical sheet in the region $|s/M^2| = 0(1)^5$. Another region of interest is where $|s/M^2| \gg 1$. In this region such a trivial example cannot be found. Therefore, restricting oneself to region $|s/M^2| \gg 1$, we will now investigate the singularity structure implied by certain class of Feynman diagrams in the ϕ^3 theory. We will notice some very important simplifications.

In the region $|s/M^2| \gg 1$, we expect that the dominating process in the inclusive reaction is the Regge exchange shown in Fig. 6. In

In particular in the case of $\pi^+ p \rightarrow \pi^+ + X$ at $M^2 = m_p^2$, Fig. 6 represents an elastic $\pi^+ p \rightarrow \pi^+ p$ process which is dominated by the Pomeron exchange. Experimentally in the reaction $p + p \rightarrow p + X$,⁷ it is seen that $I = 1/2$ baryon resonances are produced and the cross section is constant in energy. Furthermore, the Δ_{33} resonance production cross section goes down rapidly with energy. This indicates that in the reaction $pp \rightarrow p + X$, Pomeron exchange gives the cross section which is constant in s and the lower lying trajectories for ρ gives the contribution which decrease in s . In fact these experiments tell us that Fig. 6 is the dominant contribution. We use this experimental result to say that in the limit of large $|s/M^2|$, only certain class of diagrams is important in the ϕ^3 theory. Consider the diagram shown in Fig. 7.

(i) The four point function associated with the lower black blob corresponds to the arbitrary sum of diagrams in the ϕ^3 theory such that it behaves as $\left[-(p_2 + k)^2\right]^{\alpha(t)} \beta(k_1^2, (k + p_2 - q)^2, t)$ in the limit of large $(p_2 + k)^2$. Similarly for the upper black blob. Furthermore, we assume that the asymptotic behavior of $\beta(m_1^2, m_2^2, t)$ on the complex m_1^2, m_2^2 plane is such that a double dispersion relation can be written. The ladder diagrams satisfy these criteria.

(ii) The checked blob is a six-point function which represents arbitrary Feynman diagrams with n number of propergators and

l number of loops.

From the experimental evidence presented above, in the limit of large s/M^2 the set of diagrams belonging to Fig. 7 gives the dominating contribution to the amplitude. We therefore restrict ourselves to these diagrams. A crucial question is whether the class of diagrams contained in Fig. 7 possesses singularities other than those required by analyticity. To answer this, we will prove a following theorem in the next section.

Theorem: In the limit of large s , the necessary condition for the diagram (Fig. 7 satisfying (i) and (ii) above) to possess complex branch points on the physical M^2 plane is that $\beta(m_1^2, m_2^2, t)$ possesses complex branch point on the m_1^2 , or m_2^2 plane or a branch point at m_1^2 or $m_2^2 \leq \mu_0^2$.

If $\beta(m_1^2, m_2^2, t)$ possesses only a cut on the real axis at $\mu_0^2 < m_1^2, m_2^2$, the analyticity of the diagram Fig. 7 can be deduced from that of Fig. 8 and only the cut due to the unitarity shown in Fig. 3 is present in the amplitude T . This theorem reduces the study of the six-point function analyticity to that of four-point Regge-residue function in this particular kinematical limit. For example, if we sum over only the leading logarithmus in the ladder diagram, $\beta(m_1^2, m_2^2, t) = \text{constant}$. Thus to this order, Fig. 7 contains cuts only on the real axis corresponding to the unitarity cut shown in Fig. 4. We feel however uneasy to restrict ourselves to the leading log since the nonleading log is also important

in obtaining the asymptotic behavior of the residue function⁷

$$\beta(m_1^2, m_2^2, t) \xrightarrow{m_1^2 \rightarrow \infty} \sqrt{(m_1^2)^\alpha(t)} \quad (9)$$

Incidentally, the asymptotic Eq. 9 does not give any complex cut on the m_1^2 plane.

IV. THEOREM

This section contains a proof of the theorem. A reader who is not interested in the detail may skip this section without losing continuity. The Feynman amplitude of Fig. 7 with ℓ loops and n propagators in the checked blob may be written as

$$F = \int \prod_{i=1}^{\ell+1} \frac{d^4 k_i}{(2\pi)^4} \frac{\beta(k_1^2, (k_1 + p_1 + q)^2, t) \beta(k_2^2, (k_2 - p_2 - q)^2, t') [- (k_1 + p_2)^2]^\alpha [- (k_2 + p_1)^2]^\alpha}{(k_1^2 - \mu_0^2) ((k_1 + p_1 + q)^2 - \mu_0^2) (k_2^2 - \mu_0^2) (k_2 - p_2 - q)^2 - \mu_0^2} \prod_{r=1}^n (q_r^2 - \mu_r^2) \quad (10)$$

where we have labeled the momenta flowing through the loops by k_i , momenta associated with the internal lines q_r and the mass of the internal particles was taken to be μ_0 .^{8,9} By the asymptotic behavior assumed above (i), we can write an integral representation

$$\begin{aligned}
 \frac{\beta(k_1^2, (k_1 + p_2 + q)^2, t)}{(k_1^2 - \mu_0^2)((k_1 + p_2 + q)^2 - \mu_0^2)} &= \int_C \frac{\tilde{\rho}(\mu_1^2, \mu_2^2, t, \mu_0^2)}{(k_1^2 - \mu_1^2)((k_1 + p_2 + q)^2 - \mu_1^2)} d\mu_1^2 d\mu_2^2 \\
 &+ \int_C \frac{\tilde{\rho}(\mu_1^2, \mu_2^2, t, \mu_0^2)}{(k_1^2 - \mu_0^2)((k_1 + p_2 + q)^2 - \mu_2^2)} d\mu_1^2 d\mu_2^2 + \int_C \frac{\tilde{\rho}(\mu_1^2, \mu_0^2, t, \mu_0^2)}{(k_1^2 - \mu_1^2)((k_1 + p_2 + q)^2 - \mu_0^2)} d\mu_1^2 d\mu_2^2 \\
 &\equiv \int_C \frac{\rho(\mu_1^2, \mu_2^2, t, \mu_0^2)}{(k_1^2 - \mu_1^2)((k_1 + p_2 + q)^2 - \mu_2^2)} d\mu_1^2 d\mu_2^2 \tag{11}
 \end{aligned}$$

Where the path of integration μ_1^2, μ_2^2 may be complex depending on the singularity structure of $\beta(m_1^2, m_2^2, t)$. Finite number of subtraction constants will not affect our argument below. Using the representation

$$\frac{(-s)^\alpha}{\sin \pi \alpha} = \frac{1}{\pi} \int \frac{(m^2)^\alpha}{s - m^2 + i\epsilon} dm^2 \tag{12}$$

which is valid for $\alpha < 0$, we can rewrite Eq. 10.

$$F \propto \int_{\mu_0^2}^{\infty} d\mu_1^2 d\mu_2^2 \rho_1(\mu_1^2, \mu_2^2, t, \mu_0^2) \rho_2(\mu_1^2, \mu_2^2, t, \mu_0^2) \int_0^{\infty} dm_1^2 dm_2^2 (m_1^2)^\alpha (m_2^2)^\alpha \left(\frac{\sin \pi \alpha}{\pi}\right)^2 G \tag{13}$$

where

$$G = \int \frac{\prod_{i=1}^{l+2} d^4 k_i}{((k_1 - g)^2 - m_1^2) (k_1^2 - \mu_1^2) ((k_1 + p_2 + g)^2 - \mu_2^2) (k_2^2 - M_3^2) ((k_1 - p_2 - g)^2 - \mu_4^2) ((k_1 + p_2)^2 - m_1^2) \prod_{r=1}^n (g_r^2 - \mu_0^2)}$$

$$= (n+5)! \int \prod_{i=1}^{l+2} d^4 k_i \prod_{j=1}^{n+6} dx_j \delta(1 - \sum_{j=1}^{n+6} x_j) \times \quad (15)$$

$$\left\{ (k_1^2 - \mu_1^2) X_3 + [(k_1 + p_2 + g)^2 - \mu_2^2] X_4 + [k_2^2 - M_3^2] X_5 + [(k_1 - p_2 - g)^2 - \mu_4^2] X_6 + [(k_1 + p_2)^2 - m_1^2] X_1 \right. \\ \left. + [(k - g)^2 - M_2^2] X_2 + \sum_{r=7}^{n+6} (g_r^2 - \mu_0^2) X_r \right\}^{n+6}$$

G is an integral involved in a diagram shown in Fig. 9.¹⁰ When the loop integration is performed in Eq. 15, we obtain

$$G \propto \int_0^1 \prod_{j=1}^{n+6} dx_j \frac{\delta(\sum_{j=1}^{n+6} x_j - 1) C^{n+4-2l}}{[D + i\epsilon C]^{n+6-2l}} \quad (16)$$

where C is a function of x 's only and ¹¹

$$D = \sum_{k=1}^6 \int_{\mathcal{K}} (x_1, \dots, x_{n+6}) \overline{m}_k^2 + \sum_{j=1}^{25} f_j(x_1, \dots, x_{n+6}) X_j \quad (17)$$

$$- \left(\sum_{r=6}^{n+6} X_r \mu_0^2 + m_1^2 X_1 + m_2^2 X_2 + \mu_1^2 X_3 + \mu_2^2 X_4 + M_3^2 X_5 + \mu_4^2 X_6 \right) C$$

x_j are all possible invariants that can be constructed out of six four

vectors. They are given in footnote 4. \bar{m}_k^2 are external masses.

With Eq. 16, m_1^2, m_2^2 integration in Eq. 13 can be performed explicitly.

Note that in order to perform this integration, it is necessary to keep

$\alpha < 0$, $D' = D + m_1^2 x_1 + m_2^2 x_2 \neq 0$. Such a region exists (e.g., where $\bar{m}_k^2 \approx 0, x_j \approx 0$) and analytical continuation to their physical values can

be performed after the integration. The result is

$$F \propto \frac{\Gamma^2(\alpha+1) \Gamma(n-2\ell+4-2\alpha)}{\Gamma^2(n-2\ell+6)} \int_{\mu_3^2}^{\infty} d\mu_1^2 d\mu_2^2 I \int^{\circ}(\mu_1^2, \mu_2^2, t, \mu_0^2) f(\mu_3^2, \mu_4^2, t, \mu_0^2) \quad (18)$$

where

$$I = e^{-2\pi i \alpha} \int_{j=1}^{n\ell} \prod d x_j \frac{C^{n+2-2\ell-2\alpha} x_1^{-\alpha-1} x_2^{-\alpha-1} \delta(\sum_{j=1}^{n\ell} x_j - 1)}{(D')^{n-2\ell+4-2\alpha}}$$

$$D' = D + m_1^2 x_1 + m_2^2 x_2 \quad (19)$$

In the forward limit and large s, we have

$$\begin{aligned}
 s &= s' = -s_2 = -s_2', \quad t = t', \quad \chi_1 = \chi_2 = \chi_3 = 0 \\
 \chi_4 = \chi_5 &= (p_b - \delta)^2, \quad \chi_6 = \chi_9 = -t + 2(m^2 + \delta^2), \\
 \chi_7 = \chi_8 &= (p_b + \delta)^2, \quad \chi_{10}, \dots, \chi_{15} = \text{masses}^2.
 \end{aligned} \tag{22}$$

Writing D' explicitly

$$\begin{aligned}
 D' &= (\tilde{f}_1 + \tilde{f}_4 + f_{11} + f_{15} + \tilde{f}_2 + \tilde{f}_5 + f_{10} + f_{12}) m^2 \\
 &+ (\tilde{f}_3 + \tilde{f}_6 + f_{13} + f_{14}) M^2 + f_4 (p_b - \delta)^2 + f_5 (p_b' - \delta)^2 \\
 &+ (f_6 + f_9) [-t + 2(m^2 + \delta^2)] + f_7 (p_b + \delta)^2 + f_8 (p_b' + \delta)^2 \\
 &+ (f_{16} - f_{20}) s + (f_{17} - f_{21}) s' + (f_{18} + f_{19}) t \\
 &+ f_{22} M^2 + f_{23} M_1^2 + f_{24} M_2^2 + f_{25} M_3^2 \\
 &- \left(\sum_{r=6}^{146} X_r M_0^2 + \mu_1^2 X_3 + \mu_2^2 X_4 + \mu_3^2 X_5 + \mu_4^2 X_6 \right) C
 \end{aligned} \tag{23}$$

The equality among the invariants in the forward limit is true only for the real part. At this stage it will be seen below that it is important to distinguish s and s' . We can simplify Eq. 23 by relation Eq. 4, the result is

$$\begin{aligned}
D' = & g_1 M^2 + g_2 s + g_3 s' + g_4 t + g_5 \mu^2 + g_6 m^2 \\
& - \left(\sum_{r=6}^{n+6} X_r \mu_0^2 + \mu_1^2 X_3 + \mu_2^2 X_4 + \mu_3^2 X_5 + \mu_4^2 X_6 \right) C
\end{aligned} \tag{24}$$

where

$$\begin{aligned}
g_1 = & (f_4 + f_5 - f_7 - f_8 + f_{22} - f_{23} - f_{24} + f_{25}) \\
g_2 = & (-f_4 + f_8 + f_{16} - f_{20} + f_{24} - f_{25}) \\
g_3 = & (-f_5 + f_7 + f_{17} - f_{21} + f_{24} - f_{25}) \\
g_4 = & (-f_4 - f_5 - f_6 + f_7 + f_8 - f_9 + f_{18} + f_{19} - 2f_{25}) \\
g_5 = & (\tilde{f}_3 + \tilde{f}_6 + f_4 + f_5 + f_7 + f_8) \\
g_6 = & (\tilde{f}_1 + \tilde{f}_2 + \tilde{f}_4 + \tilde{f}_6 + 2f_4 + 2f_5 + 2f_6 + 2f_9 + f_{10} + f_{11} \\
& + f_{12} + f_{15} + 2f_{23} + 6f_{25})_0.
\end{aligned}$$

Eq. 18 with D' function given by Eq. 24 is a general form of the amplitude.

We are interested in a particular kinematical region, namely large s and s' , and s is evaluated on upper side of the cut in s , s' is evaluated on the lower side of the cut in s' , and $t \leq 0$. We can not simply take the large s limit of Eq. 18 along the real axis since the integral representation Eq. 18 is not defined there. In order to get around this point, we define function h_2 and h_3

$$g_2(X_1, \dots, X_{n+6}) = X_1 h_2(X_2, \dots, X_{n+6})$$

$$g_3(X_1, \dots, X_{n+6}) = X_2 h_3(X_1, X_3, \dots, X_{n+6})$$

(We note that $f_j \propto x_1$ for $j = 1, 3, 4, 6, 8, 9, 10, 11, 12, 13, 16, 21, 24, 25$ and $f_j \propto X_2$ for $j = 1, 3, 5, 6, 7, 9, 10, 12, 14, 15, 17, 20, 24, 25$. These follow since we must cut the line associated with x_1 or x_2 to form the invariants χ_j listed in the footnote 4.) We divide the integration region of Eq. 16 into four parts by inserting

$$[\theta(h_2) + \theta(-h_2)][\theta(h_3) + \theta(-h_3)] = 1 \tag{25}$$

into the Eq. 16. Later we will be looking for a term proportional to $s^{2\alpha}$ which comes from outside the region where $h_1, h_2 \gg \left|\frac{1}{s}\right|$.

Therefore, we can write I as sum of four integrals. (If the integration region where h_2 or $h_3 \approx 0$ is important, then it required extra care.)

Calling I_1, \dots, I_4 terms with $\theta(h_2)\theta(h_3), \theta(h_2)\theta(-h_3), \theta(-h_2)\theta(h_3),$ and $\theta(-h_2)\theta(-h_3)$ respectively. We see that I_1 has cuts when $s, s' > 0$, I_2 has cuts when $s > 0, s' < 0$, I_3 and I_4 have cuts when $s < 0, s > 0$ and $s < 0, s' < 0$, respectively. Therefore large s, s' limit can be taken in the direction where it is regular in s and s' , that is $s, s' \rightarrow -\infty$ for $I_1, s \rightarrow -\infty, s' \rightarrow \infty$ for I_2 , etc. We will demonstrate the technique for I_1 . The technique can be applied for I_2, \dots, I_4 also. Writing

$$I_1 = e^{-2\pi i \alpha} \int_{\mathcal{D}} \prod_{j=1}^{n+6} dx_j \frac{\delta(\sum_{j=1}^{n+6} x_j - 1) C^{n+2-2\alpha-2\alpha} \theta(h_2)\theta(h_3) x_1^{-\alpha-1} x_2^{-\alpha-1}}{D^{n+2\alpha+4-2\alpha}} \tag{26}$$

We take the large s, s' limit of Eq. 26. Note, however, that Eq. 26 converges only for $\alpha < 0$. Therefore, what we must do is to single out the region of integration where I_1 behaves like $s^\alpha s'^{-\alpha}$ and analytically continue to $\alpha < 0$ after doing the integration explicitly.

Note that for $\alpha < 0$, such a term is not the leading term. Furthermore, when $s, s' \rightarrow \infty$, the integral representation ceases to be valid since I_1 will diverge when s, s' reaches the threshold value for their respective channels. When all other invariants are kept below threshold, in particular negative, integral is well defined when $s, s' \rightarrow \infty$. I_1 is well defined on the upper half s and s' planes as well as on the negative real axis, and therefore using Schwartz reflection principle, it is analytic on the physical sheet of s and s' plane except for the cut on the real positive axis. Therefore, we can continue $s, s' \rightarrow -\infty$ limit to obtain $s \rightarrow \infty + i\epsilon$ and $s' \rightarrow \infty - i\epsilon$.

(Assumption about the real integration range for μ_1, \dots, μ_4 is important here.) Note the presence of $x_1^{-\alpha-1}, x_2^{-\alpha-1}$ in the numerator of Eq. 26. When s and s' are large, the integration region $x_1 \sim |1/s|, x_2 \sim |1/s'|$ gives the dominant contribution proportional to $s^\alpha s'^{-\alpha}$. When

h_1 or $h_2 \sim |1/s|$, the contribution proportional to $s^\alpha s'^{-\alpha}$ does not arise. Therefore, we can restrict ourselves to the region $h_1, h_2 \gg |1/s|$.

This justifies the splitting of I into I_1, \dots, I_4 . First we fix $s' < 0$ and take $s \rightarrow -\infty$. Setting $y = x_1 sh_1/R,$

$$I_1 = (-S)^\alpha e^{-i\pi\alpha} \int_0^{sh_1/R} dy \prod_{j=2}^{n+6} dx_j \delta\left(\sum_{j=2}^{n+6} x_j - 1\right) \frac{C^{n+2-2\ell-2\alpha} \theta(h_1) \theta(h_2) h_1^\alpha y_1^{-\alpha-1} x_2^{-\alpha-1}}{R^{n-2\ell+4-\alpha} [1+y]^{n-2\ell+4-2\alpha}}$$

(27)

where $R = D - sg_2$. In taking the larger s limit, the x_1 appearing in R as well as in the s function and c can be set to zero. i. e., f_j , $j = 1, 3, 4, 6, 8, 9, 10, 11, 12, 13, 21, 24, 25$ drops out of the problem. In particular, we note that f_4, f_8, f_{24}, f_{25} corresponding to M_2, M_3, χ_4, χ_8 drop out. So Eq. 27, for large s , does not contain singularities from channels shown in Fig. 3c, d, e, h. (Later we will see that when large s limit is taken, the limiting expression does not contain the singularities from channels shown in Fig. 3f, g and contains only those in Fig. 3a, b.) Note that the path of integration depends on what we take for the phase of sh_1/R . The singularity of the integrand at $y = -1$ never makes the integral diverge. In fact we take the path of integration shown in Fig. 10. Since the value of integral is zero everywhere except along the positive real axis,

$$I_1 \approx (-s)^\alpha e^{-i\pi\alpha} \frac{\Gamma(-\alpha)\Gamma(n-2l+4-\alpha)}{\Gamma(n-2l+4-2\alpha)} \int_{j=2}^{n+6} \frac{\pi dx_j}{\pi} C \frac{\Theta(h_1)\Theta(h_2) h_1^\alpha h_2^{\alpha-1}}{(R')^{n-2l+4-\alpha}}$$

(28)

$$R' = [R]_{x_i=0} .$$

The large s' limit can be taken in the same way. Continuing to the region $\alpha > 0$, and continuing s and s' from the negative axis to $s_0 + i\epsilon$ and $s_0 - i\epsilon$ respectively along the positive real axis, we have

$$I_1 \approx \frac{|s|^{2\alpha} \Gamma^2(-\alpha) \Gamma(n-2l+4)}{\Gamma(n-2l+4-2\alpha)} \int_{j=3}^{n+6} \frac{\pi dx_j}{\pi} C \frac{\Theta(h_1)\Theta(h_2) h_1^\alpha h_2^\alpha}{k^{n-2l+4}}$$

(29)

where

$$k = (f_{22} - f_{23}) M^2 + (f_{18} + f_{19}) t + (\tilde{f}_1 + \tilde{f}_2 + \tilde{f}_4 + \tilde{f}_5 + 2f_{23}) m^2 - \left(\sum_{r=6}^{n+6} x_r \mu_0^r + \mu_1^2 x_3 + \mu_2^2 x_4 + \mu_3^2 x_5 + \mu_4^2 x_6 \right) C$$

(30)

All invariants which were multiplied by x_1 and x_2 were eliminated.

Finally,

$$\begin{aligned}
 F \propto |s|^{2\alpha} \frac{\Gamma(n+4-2\alpha)}{\Gamma^2(n-2\alpha+6)} \frac{\pi^2}{2\mu_0^2 \Gamma\alpha} \int_C \prod_{i=1}^4 d\mu_i \Theta(h_1) \Theta(h_2) K^{-n+2\alpha-4} \\
 \times \int_1^{\mu_1^2} (\mu_1^2, \mu_2^2, t, \mu_0^2) \int_2^{\mu_4^2} (\mu_3^2, \mu_4^2, t, \mu_0^2) h_1(x_3, \dots, x_{n+6}) h_2(x_3, \dots, x_{n+6}) C^{n-2\alpha-2\alpha+2}
 \end{aligned}
 \tag{31}$$

where the subscript 1 corresponds to the contribution of I_1 to F . Assuming that μ_i integrations are on the real axis $\mu_i^2 > \mu_0^2/2$, we can deduce the analyticity of F on the M^2 plane from Eqs. 30 and 31. Note that K is exactly the denominator function for the four point function when two of the external particle has mass t . Since the region $x_1 \sim 1/s$, $x_2 \sim 1/s'$ gives the contribution, it can be represented by Fig. 11. The four-point function to arbitrary order in the coupling constant has been discussed in many places.^{12,13} The only possible additional complication in our problem is that two of the masses are $t < 0$, and that some of the internal masses μ_1, \dots, μ_4 are integrated from μ_0^2 to ∞ . But we note that Ref. 13 shows that the propagator is negative definite below threshold when all the external particles are on their mass shell. The continuation from their mass shell to $t < 0$ will make the denominator more negative. Same is true for any $\mu_i^2 > \mu_0^2$. Since the integral over μ_i^2 are convergent, we see that F is analytic on the upper half M^2 plane as well as $M^2 < 4\mu_0^2$ on the real axis. Then the Schwartz reflection principle can be used to see that F is analytic everywhere on the physical sheet $M^2 \geq 4\mu_0^2$ on the real axis. Note that

these arguments will be false if μ_i^2 is complex, that is if the residue function $\beta(m_1^2, m_2^2, t)$ has a singularity on the complex m_1^2, m_2^2 plane.

IV. SUM RULE

The theorem states that if there is any complex branch point, the source of such a branch point is in the Regge residue function of the ordinary two-to-two scattering amplitude. We are not prepared, here, to make any statement about the Regge-residue function. We would rather take the point of view that if the results of assuming no complex branch point on the M^2 plane does not agree with experiment then we know a possible source of the problem.

In this section, we assume that no other branch point except those coming from unitarity exists. The singularity structure for I, is shown in Fig. 12. (For those who skipped Section IV, I, is the part of T which contains all the leading singularities in the limit of large s.) The discontinuity across the cut, according to Eq. 6 is proportional to the inclusive cross section. Therefore, if we know the M^2 dependence of the amplitude around the circle of radius M_0^2 , we can use the formula

$$\oint (M^2)^n I \downarrow M^2 = 0 \quad (32)$$

to obtain the relationship between experimentally measurable quantities.¹⁴

The triple Regge expansion supplies the M^2 dependence around the circular contour. According to the triple Regge expansion we have

$$T \xrightarrow[M^2 \rightarrow \infty]{S/M^2 \rightarrow \dots} \frac{\pi}{4 m^2} \sum_{ijk} \left\{ \eta_j \eta_k^* \left(\frac{S}{M^2}\right)^{\alpha_j(t) + \alpha_k(t)} (M^2)^{\alpha_i(0)} \frac{\beta_{bbi}(t) g_{ijk}(t) S_i}{\sin \pi (\alpha_i(0) - \alpha_j(t) - \alpha_k(t))} + \sum_r F_{ijk}^r \right\} \quad (33)$$

where

$$\eta_j = \beta_{acj}(t) \frac{e^{-i\pi\alpha_j(t)} \pm 1}{\sin \pi \alpha_j(t)}, \quad S_i = e^{-i\pi(\alpha_i(0) - \alpha_j(t) - \alpha_k(t))} + 1$$

$\beta_{abj}(t)$ is a Regge-residue function associated with particle a, b and

Regge trajectory j coupling, $g_{ijk}(t)$ is the triple-Regge residue function.

They are normalized in the same way as Ref. 15. These notations are defined by Fig. 13. In particular our $g_{\text{PPP}}(t)$ where P stands for the

Pomeron, corresponds to $g_p(t)$ in Ref. 15. $\alpha(0)$ and $\alpha_j(t)$ are the

Regge trajectory functions. When $\alpha_i(0) - \alpha_j(t) - \alpha_k(t) = \gamma = \text{integer}$, the

first term of Eq. 33 seems to have spurious poles. They are cancelled

by either (i) zero in $g_{ijk}(t)$ or (ii) by F_{ijk}^r . The spurious poles have been

studied in Ref. 10 by computing a particular Feynman diagram in the

ϕ^3 theory. It was found that for $\gamma \leq 0$, $F_{ijk}^n = 0$ and $g_{ijk}(t)$ has a zero,

for $\gamma \geq 1$, F_{ijk}^n is present to cancel the poles. It is therefore, quite

reasonable to assume that $F_{ijk}^n = 0$ for $n \leq 0$. For $n \geq 1$, F_{ijk}^n is a

polynomial and even if it is present,

$$\oint F_{ijk}^r (M^2)^n dM^2 = 0$$

and gives no contribution to Eq. 32. Using Eq. 6 and argument on the left hand cut presented in Sec. II, we obtain

$$\begin{aligned} & \int_{m^2}^{M_0^2} (M^2)^n \frac{d\sigma}{dt dM^2} \Big|_{a+b \rightarrow c+x} dM^2 - (-1)^n \int_{m^2}^{M_0^2} (M^2)^n \frac{d\sigma}{dt dM^2} \Big|_{c+b \rightarrow a+x} dM^2 \\ &= \sum_{ijk} (1 - (-1)^n) \frac{\eta_j \eta_k^*}{16 \pi S^2} \left(\frac{S}{M_0^2}\right)^{\alpha_j(t) - \alpha_k(t)} (M_0^2)^{\alpha_i(c) + n + 1} \frac{\beta_{bb_i}(c) g_{ij^*}(z)}{\alpha_i(c) - \alpha_j(t) - \alpha_k(t) + n + 1} \end{aligned} \tag{34}$$

Note that only even signatured Regge poles contribute in "i". This is because the inclusive cross section is always symmetric in j and k.

It is important to point out that for $\left. \frac{d\sigma}{dt dM^2} \right|_{c+b \rightarrow a+x}$

The center of mass squared of b and c is

$$(p_b + p_c)^2 = S + \mu^2 - M^2 + t$$

and it is not fixed along the integration path. When major contribution to the integral comes from lower end of the integral, however, modification due to the energy shift should be small. Note also that if $a = c$, Eq. 34 reduces to a trivial equation for even n.

V. EXTENSIONS¹⁶

Eq. 34 in general requires measurements of two inclusive cross section $a+b \rightarrow c+X$ and $c+b \rightarrow a+X$. In this section we discuss sum rules which stem from Eq. 34 but require less experimental data. We see immediately that for $a = c$ and odd n we have

$$\int_{m^2}^{M_i^2} (M^2)^n \frac{d\sigma}{dt dM^2} \Big|_{a+b \rightarrow c+X} = \sum \frac{1}{16\pi s^2} \left(\frac{s}{M^2}\right)^{\alpha_j(t) + \alpha_k(t)} \frac{\alpha_i(t) + n + 1}{(M^2)^{n+1}}$$

$$\times \frac{\beta_{bba}(0) g_{ijk}(t)}{\alpha_i(0) - \alpha_j(t) - \alpha_k(t) + n + 1}$$

(35)

where the sum "i" runs over only even signatred trajectories.

The contribution from the cross channel $c + b \rightarrow a + X$ in Eq. 34 comes from the fact that I contains both right and left hand cuts.

Suppose now that we can make the separation

where I_R (I_L) is an analytic function of s , t , and M^2 which contains only the right (left) hand cut on the M^2 plane in the limit of large s and fixed t . Let us further assume that they both have a triple-Regge behavior with appropriate phase factors. (i. e. no fixed poles) sum rule can be written for both I_L and I_R separately and we obtain

$$\int_{m^2}^{M_0^2} (M^2)^n \frac{d\sigma}{dt dM^2} \Big|_{a+b \rightarrow c+x} dM^2 = \sum_{j,k} \frac{1}{16\pi S^2} \eta_j \eta_k^* \left(\frac{S}{M_0^2}\right)^{\alpha_j(t) + \alpha_k(t)} (M_0^2)^{\alpha_j + n + 1} \frac{\beta_{bbi} g_{ijk}(t)}{\alpha_i(0) - \alpha_j(t) - \alpha_k(t) + n + 1} \quad (37)$$

Let us now discuss the content of this sum rule. (a) Consider a reaction $a + b \rightarrow a + x$. Then the leading Regge trajectory is $i = j = k =$ Pomeranchuk. For $n = 0$, and small t , we can write

$$\int_{m^2}^{M_0^2} \frac{d\sigma}{dt dM^2} \Big|_{a+b \rightarrow a+x} dM^2 = \frac{1}{16\pi} \frac{\beta_{bbp} |\beta_{acp}|^2 g_{PPP}(t)}{1 - \alpha_p(0) - 2\alpha' t} + \dots \quad (38)$$

where α' is the slope of the Pomeranchuk trajectory. If $\alpha_p(0) = 1$, $g_{PPP}(t)$ must have a zero at $t = 0$. The presence of this zero is well known. (b) Note that the left hand side of the sum rule (37) contains the integral over the low missing mass region and thus it contains the integral over the resonances. We might, therefore, expect that the

concept of duality from two-to-two scattering amplitude to appear here in its generalized form. This will be true if the sum rule holds for unusually low M_0^2 with only the leading Regge trajectory in the sum over i . Since the generalized form of duality is widely accepted without any experimental bases, this is a good opportunity to check it. There is also a related question concerning how the Pomeron and the ordinary Regge contributions should be related to the contributions from the resonance and the background. If we take the analogy with the two-particle scattering, we associate the contribution of the background in the M^2 channel with the Pomeron contribution in i and the contribution of the resonance with the ordinary Regge contribution in i . All these can be checked when the data in various reactions become available.

(c) For now, we associate the Pomeron contribution to the left hand side of Eq. 35. Then we obtain

$$g_{PPP}(t) = \frac{16\pi(1-\alpha_P(0)+2\alpha'(t))}{\sigma_a \sqrt{\sigma_b}} \int_{m^2}^{M_0^2} dM^2 \left[\frac{d\sigma}{d^2 + dM^2} (a+b \rightarrow a+x) \right]_{b.g.}$$

where the right side is to include only that background contribution

which has $s^{2\alpha_P(t)}$ behavior. This equation is useful for obtaining the

value for the triple-Pomeron vertex function. Note that Eq. 39 is the most reliable way to obtain $g_{PPP}(t)$. The only other way known at present

is to measure the differential cross section in the triple-Regge region. But the cross section is bound to be small due to the zero in $g_{PPP}(t)$ at $t = 0$ discussed above, and away from $t = 0$, the contribution from cuts may play a role. Another advantage of Eq. 39 is that if the background can be properly separated from the resonance, the knowledge of the low energy cross section will put a lower bound on $g_{PPP}(t)$.

Furthermore, note that factorization implies that the right hand side of Eq. 39 is a universal function of t for any a and b . A test of the universality can be made in, for example,

$$p + p \rightarrow p + x, \pi^\pm + He \rightarrow He + x, \pi^\pm + p \rightarrow p + x, \pi^\pm + p \rightarrow \pi^\pm + x, \\ K^\pm + p \rightarrow p + x, K^\pm + p \rightarrow K^\pm + x, p + \bar{p} \rightarrow p + x, \bar{p} + p \rightarrow p + x, \text{ etc. } \dots$$

The Regge behavior for the unsigned amplitudes I_R, I_L were assumed in order to obtain the above results. The verification of this assumption is, in itself, extremely interesting. We will illustrate a possibility that the fix pole may exist by a heuristic argument. Consider a Regge + particle \rightarrow Regge + particle scattering where initial Regge trajectory has spin α_k and the final Regge trajectory has spin α_j . The particle is taken to be spinless. Let the square of the direct channel energy be M^2 . Then at large M^2 , the maximum spin flip amplitude behaves as $(M^2)^{\alpha_i - \alpha_j - \alpha_k}$ where α_i is the Regge trajectory exchanged in the t channel. For example if $\alpha_j = \alpha_k = 1$, the kinematics is same as that of Compton scattering and α_i is a Pomeron. In fact, at $\alpha_i = \alpha_j = \alpha_k = 1$, the spin flip amplitude chooses wrong-signature

nonsense. In the Compton scattering one needs a fixed pole at this point in order to prevent the Pomeron from decoupling. The triple-Pomeron contribution resembles this possibility. Since the triple Pomeron decouples at $t = 0$, it may be an indication that the fixed pole corresponding to the Pomeron in the Compton scattering is absent. But it is quite possible that a fixed pole associated with other trajectories may exist.

VI. CONCLUSION

The analyticity of a scattering amplitude has been proven to be a powerful tool in understanding two-to-two reactions. The possibility of using such a tool to three-to-three amplitude becomes exceedingly complicated. We have demonstrated that in the region $|s/M^2| \gg 1$, there is a good chance that the analyticity of the three-to-three amplitude on the M^2 plane becomes very simple.

Using this analyticity, we have written a sum rule Eq. 34. This sum rule enables us to evaluate the triple-Regge residue function from a low missing mass inclusive cross section data. Such information will be very useful for future experiments at NAL.

The successes of the sum rules written here, when they are compared with experiment, will be quite significant. It means that we can apply the techniques used in the two particle scattering to the analysis of inclusive reactions. If the idea of duality in the generalized form is verified through these sum rules, we should gain confidence in the significance of dual models. In order to compare the sum rules with experiments, we need to separate the resonance and background. This is very difficult in the existing experimental data (for example Ref. 5). It is clear that future experiments should be designed such that the separation can be easily achieved. Furthermore, when $a + b \rightarrow a + X$ is being

measured, $\bar{a} + b \rightarrow \bar{a} + X$ or $a + \bar{b} \rightarrow a + X$ should be measured simultaneously.

ACKNOWLEDGEMENTS

We would like to thank L. Balazs, S. D. Ellis, D. Gordon, and J. Sullivan for discussions. We also thank S. D. Ellis and E. Paschos for reading the manuscript.

REFERENCES AND FOOTNOTES

¹A. H. Mueller, Phys. Rev. D2, 2963 (1970).

²Ref. 1 and also C. E. DeTar et al. Phys. Rev. Letters.

³H. P. Stapp, Berkeley Preprint UCRL-20623 (1971).

⁴For future reference, we list them.

$$\begin{aligned}
 \chi_1 &= (p_a - p'_a)^2, \chi_2 = (p_b - p'_b)^2, \chi_3 = (q - q')^2, \chi_4 = (p_b - q)^2, \\
 \chi_5 &= (p'_b - q')^2, \chi_6 = (p_a + q')^2, \chi_7 = (p_b + q')^2, \chi_8 = (p'_b + q)^2, \\
 \chi_9 &= (p'_a + q)^2, \chi_{10} = (p_a + p_b - p'_a)^2, \chi_{11} = (p_a + p_b - p'_b)^2, \\
 \chi_{12} &= (p_b - q + q')^2, \chi_{13} = (p_a + q' - p'_a)^2, \chi_{14} = (p_b - p'_b + q')^2, \\
 \chi_{15} &= (p_b - p'_a - p'_b)^2, s = (p_a + p_b)^2 \equiv \chi_{16}, s' = (p'_a + p'_b)^2 \equiv \chi_{17}, \\
 t &= (p_a - q)^2 \equiv \chi_{18}, t' = (p'_a - q')^2 \equiv \chi_{19}, s_2 = (p_b - p'_a)^2 \equiv \chi_{20}, \\
 s'_2 &= (p'_b - p'_a)^2 \equiv \chi_{21}, M^2 = (p_a + p_b - q)^2 \equiv \chi_{22}, \\
 M_1^2 &= (p_a - p'_b - q)^2 \equiv \chi_{23}, M_2^2 = (p_a + p_b - q')^2 \equiv \chi_{24}, \\
 M_3^2 &= (-p'_a + p_b - q)^2 \equiv \chi_{25}.
 \end{aligned}$$

⁵This part of the argument is due to Stapp Ref. 3.

⁶C-I Tan, Brown University Preprint NYO-2262 TA-240 (1971),

R. C. Hwa, Phys. Rev. 134 B1086 (1964).

⁷E. W. Anderson et al. Phys. Rev. Letters 16 855 (1966).

⁸See for example G. Tiktopoulos and S. B. Treiman Phys. Rev. 135

B711 and 136 B1217 (1964).

⁹We have put in the form $\beta [-(k_1 + p_2)^2]^\alpha$ as the contribution from the black blob. Later, we will see that the largest contribution comes

from the region where $(k_1 + p_2)^2$ is large and thus the short cut will be justified.

¹⁰The method used here is same as those used in S. -J. Chang et al. NAL preprint THY-16 (1971).

¹¹Taking Eq. 15 and performing the m_1^2 , m_2^2 integrations one can show that the term $s^2 \alpha$ comes from the region of k integration where $(k_1 + p_2)^2 = (k' - q')^2 \cong s$. Thus the discussion in footnote 7 is justified.

¹²Eden, Landshoff, Olive and Polkinghorne, The Analytic S-Matrix, Cambridge University Press (1966).

¹³J. Bjorken and S. Drell, Relativistic Quantum Fields, McGraw-Hill, New York (1965).

¹⁴While this work was in progress, the author has received M. Einhorn Berkeley Preprint UCRL-20688 (1971), Olssen CERN Preprint Th 1376 (1971), both of which discuss finite-energy sum rule to some extent.

¹⁵H. D. Abarbanel et al. Phys. Rev. Letters 26 937 (1971).

¹⁶Numerical evaluation of these sum rules is in progress. S.D. Ellis and A.I. Sanda to be published. We would like to acknowledge S. Ellis for discussions which no doubt greatly influenced the development of the material presented in this section.

FIGURE CAPTIONS

Fig. 1 Diagram for an inclusive process.

Fig. 2 Diagram for a six-point function.

Fig. 3 When s and t are fixed, any of these channels have singularities on the M^2 plane.

Fig. 4 The singularities of channels M^2 and M_1^2 on the M^2 plane. The reaction in the M^2 channel is $\pi^- p \rightarrow K^- + X$.

Position of the singularities are: $\pi^- + p \rightarrow K^- + X$

1. Physical region for $\pi^- + p \rightarrow K^- + X$, $(m_p + \mu_K)^2 \leq M^2 < (\sqrt{s} - \mu_K)^2$

2. Physical region for $K^+ \pi^- p \rightarrow X$, $(\sqrt{s} + \mu_K)^2 \leq M^2$

3. Physical region for $K^- p \rightarrow \pi^- + \Sigma$, $M^2 = 2t + 2m_\Sigma^2 - m_\Sigma^2$

4. Physical region for $K^- p \rightarrow \pi^- + X$,

$$2t + 2m - (\sqrt{s} - \mu)^2 \leq M^2 \leq 2t + 2m - (m_\Sigma + \mu_\pi)^2$$

5. Physical region for $K^- p \pi^+ \rightarrow X$, $M^2 \leq 2t + 2m^2 - (\sqrt{s} + \mu)^2$

Fig. 5 The box diagram which gives complex singularity in the physical sheet.

Fig. 6 The dominant diagram in the inclusive reaction at small t and $|s/M^2| \gg 1$.

Fig. 7 The class of diagrams in ϕ^3 theory that were studied. It has a following property:

- (i) The four point function associated with the lower black blob corresponds to the arbitrary sum of diagrams in

the ϕ^3 theory such that it behaves as

$[-(p_2+k)^2]^{-\alpha(t)} \beta(k_1^2, (k+p_2-q)^2, t)$ in the limit of large $(p_2+k)^2$. Similarly for the upper black blob.

- (ii) The checked blob is a six-point function which represents an arbitrary Feynman diagram with n number of propagators and ℓ number of loops.

Fig. 8 The diagram whose Feynman denominator function is same as that of Fig. 7 in the limit of large s .

Fig. 9 Diagram for G defined by Eq. 14.

Fig. 10 Path of integration for Eq. 27.

Fig. 11 The diagram which gives the s^α, s'^α limit when s, s' are large.

Fig. 12 Analyticity of I , on M^2 plane and the path of integration to obtain the finite-energy sum rule.

Fig. 13 The triple Regge diagram.

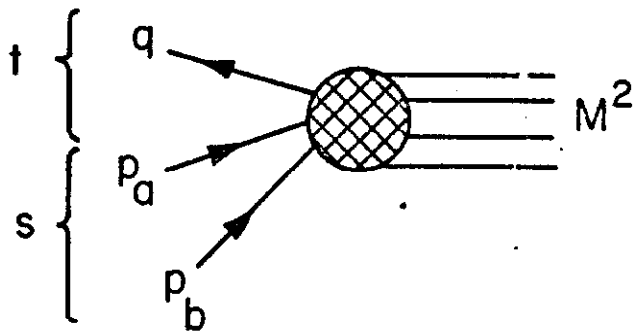


Fig. 1

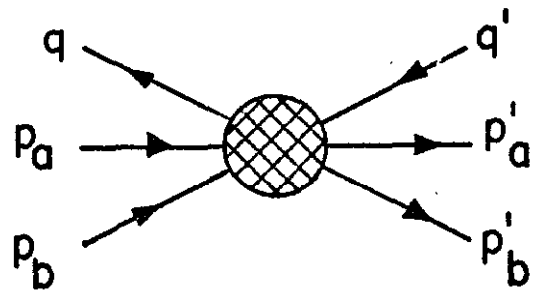


Fig. 2

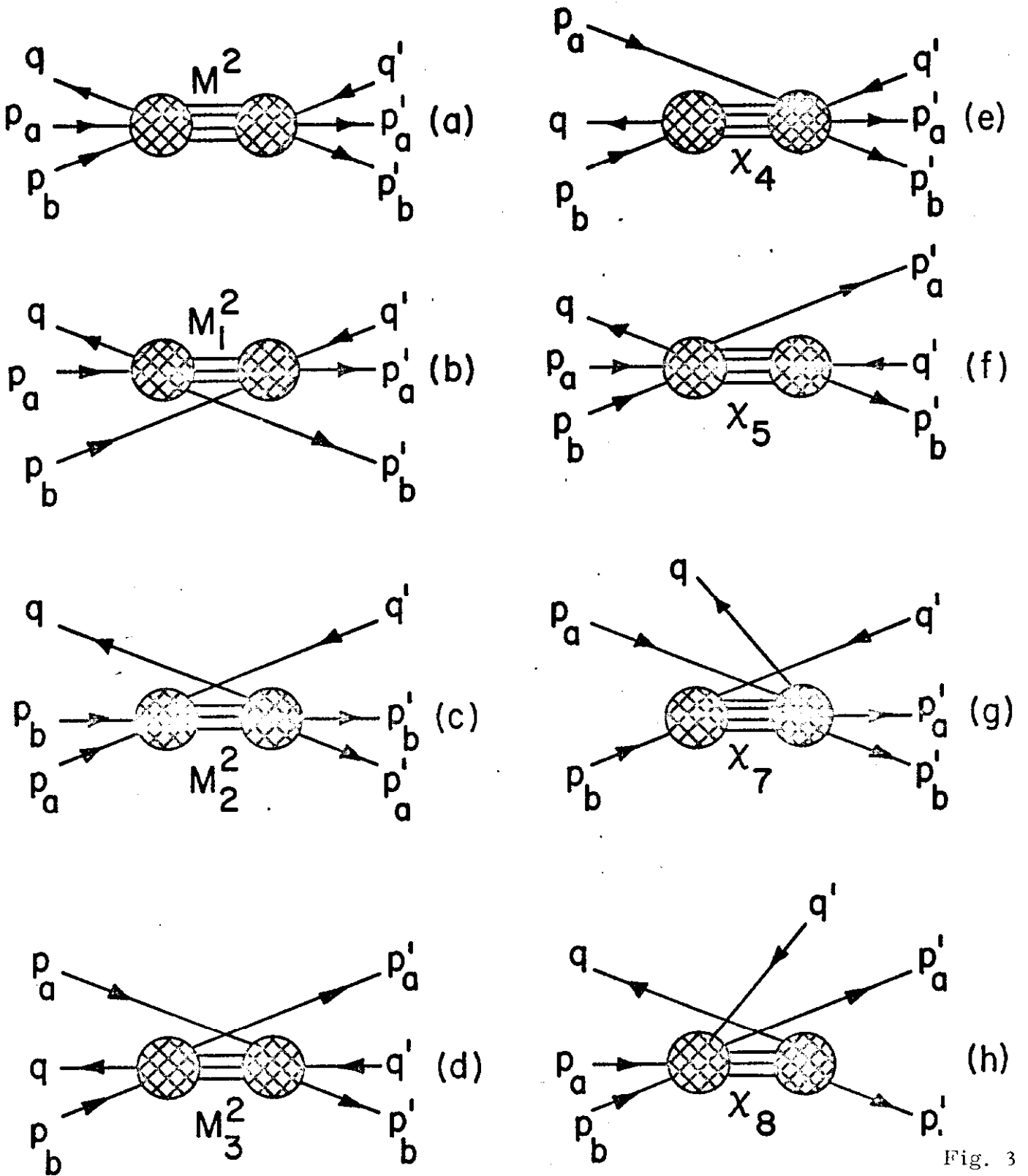


Fig. 3

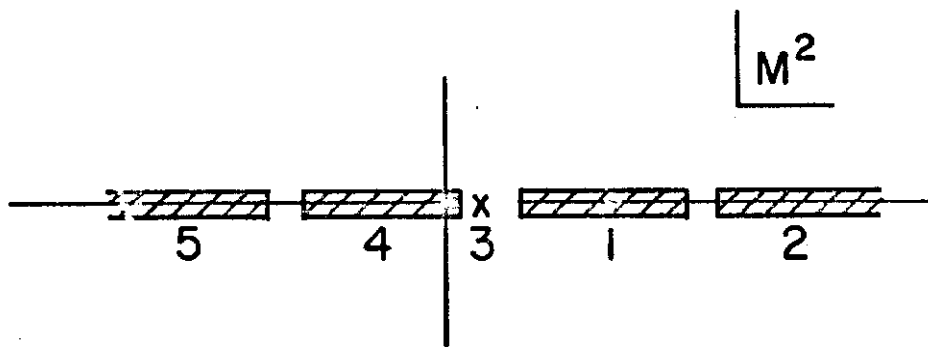


Fig. 4

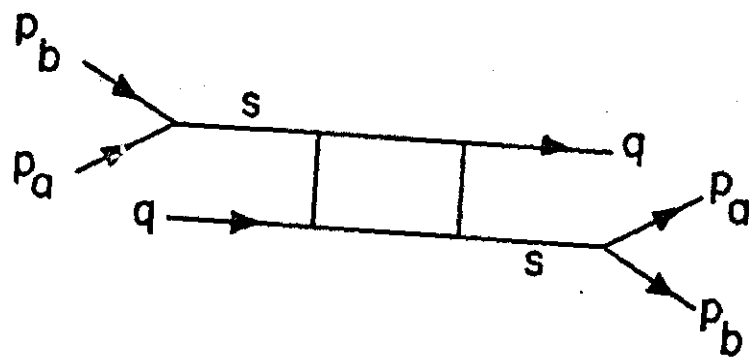
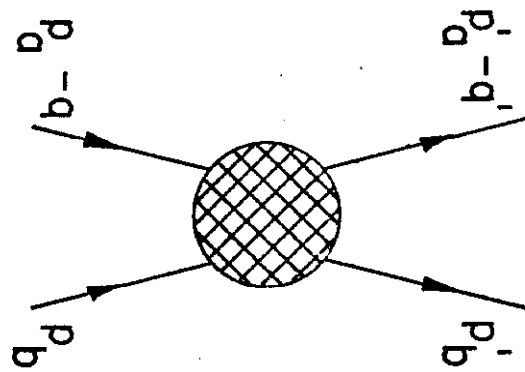
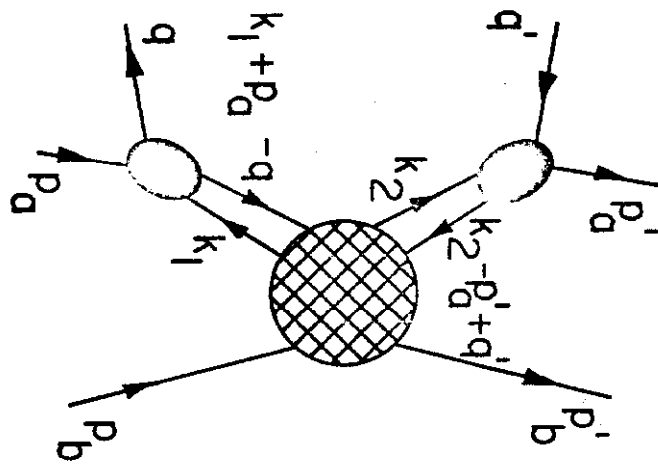
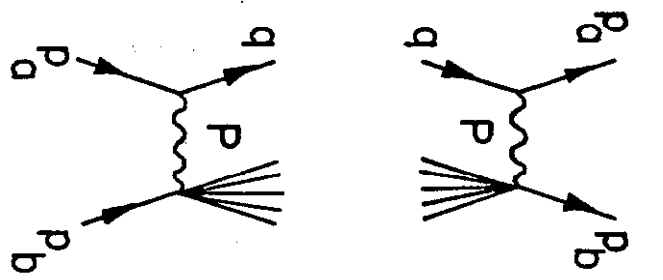


Fig. 5



Figs. 6, 7, 8

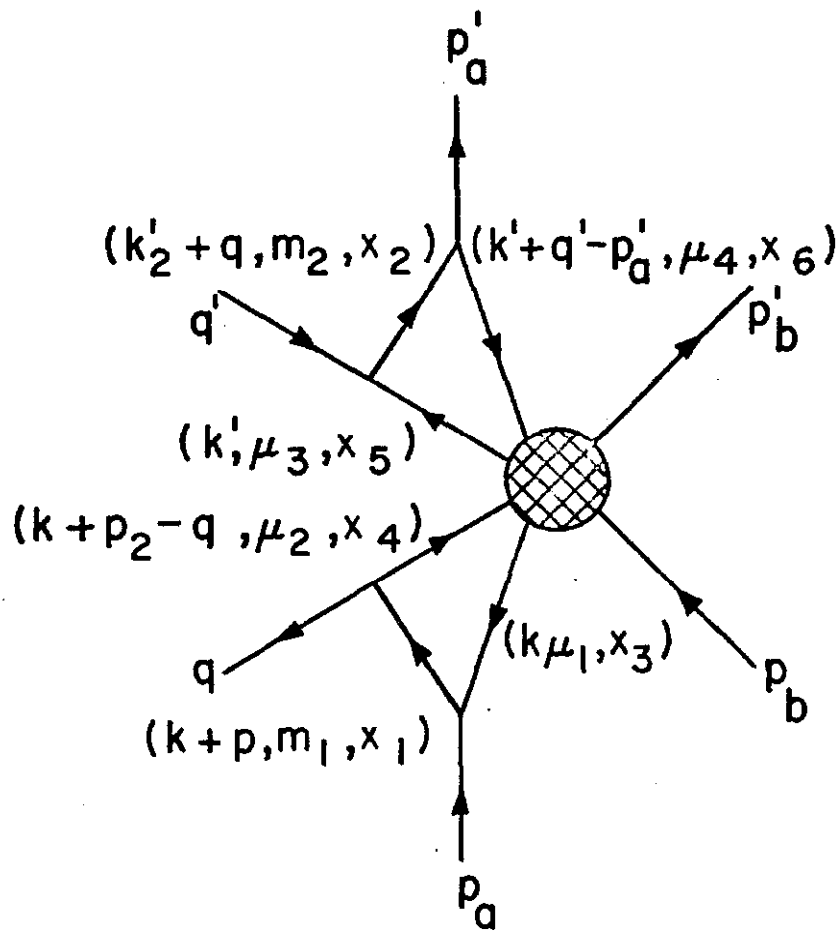


Fig. 9

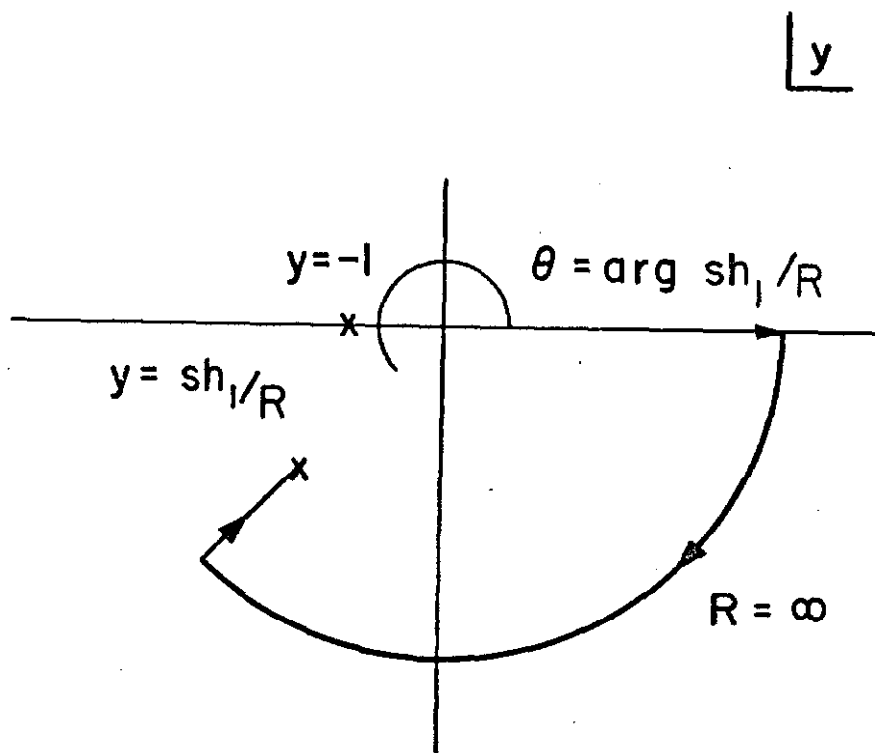


Fig. 10

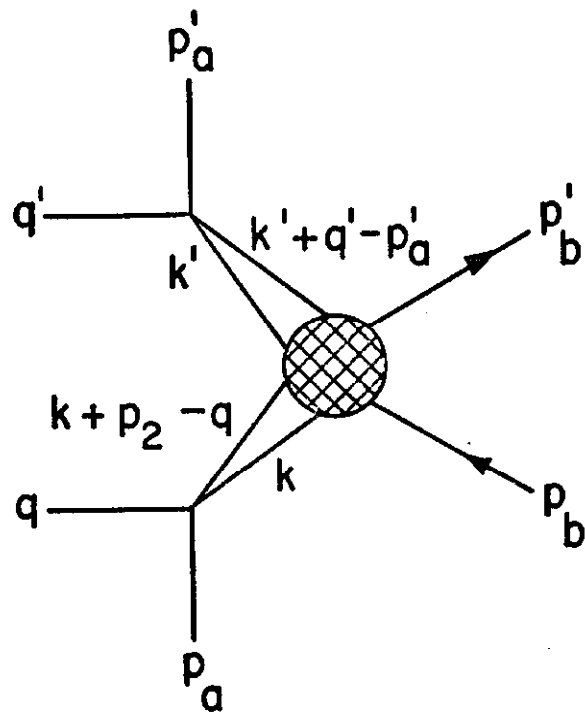


Fig. 11

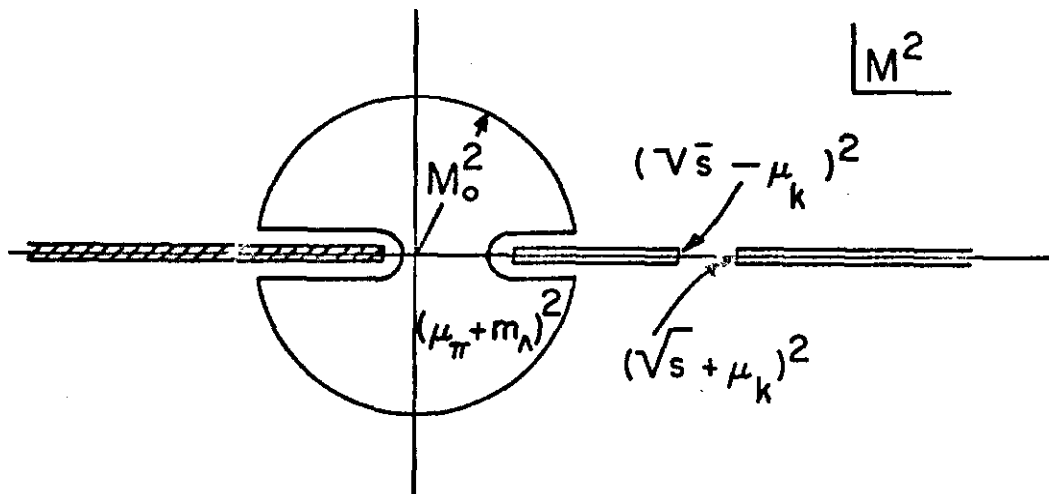


Fig. 12

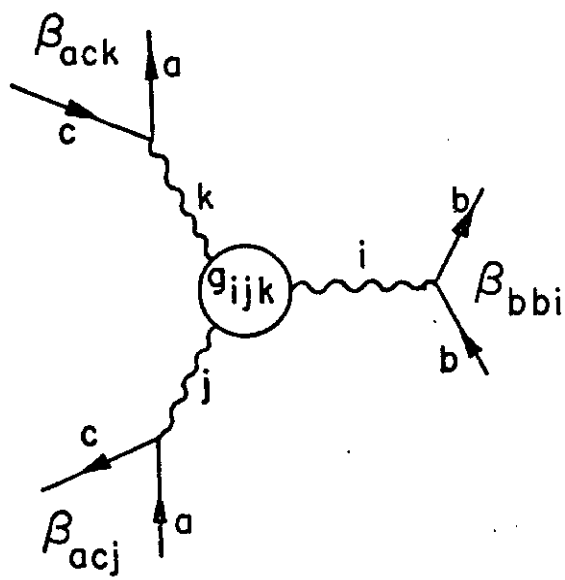


Fig. 13

Note added: We have examined $pp \rightarrow p + x$ (Ref. 7

and Alaby et. al. CERN 70-16 (1970) and $\pi - p \rightarrow p + x$

(CERN-IHEP collaboration). Following conclusions were

reached: (a) the cross sections are consistent with two

term tripple-Regge expansion

$$\frac{d\sigma}{dt dM^2} = \frac{m^2}{(16\pi)^2 s^2} \left[G_{PPf} \left(\frac{s}{M^2} \right)^{2\alpha_P(t)} \left(M^2 \right)^{\alpha_f(0)} \right. \\ \left. + G_{ffP} \left(\frac{s}{M^2} \right)^{2\alpha_f(t)} \left(M^2 \right)^{\alpha_p(0)} \right]$$

G_{PPf} and G_{ffP} are products of g, β, η , see S. D.

Ellis and A. I. Sanda, NAL-THY-30 submitted to

Phys. Rev. Letters; (b) the finite-energy sum rule

for inclusive reaction Eq. (32) is indeed satisfied.

See S. D. Ellis and A. I. Sanda NAL-THY-47.